Heterocyclic Letters
Vol. 13| No.1|143-156|November -January|2023
ISSN : (print) 2231–3087 / (online) 2230-9632
CODEN: HLEEAI
http://heteroletters.org

DESIGN, SYNTHESIS OF N-(4-(3-BROMOPHENYL)THIAZOL-2-YL)-1-AZAHETERYL CARBOXAMIDES AND THEIR ANTICANCER EVALUATION AGAINST MCF-7 CELL LINE

V. Krishna Chaitanya[a,e], P. Jalapathi*[b], M. Ravi Chandar[c], T. Vishnu[d]

[a]Department of Chemistry, Jawaharlal Nehru Technological University Hyderabad, College of Engineering, Kukatpally, Hyderabad, 500085, Telangana, India.
*[*b]Department of Chemistry, Osmania University, Hyderabad, 500007, Telangana, India.*
[c]Department of Chemistry, Mahatma Gandhi Institute of Technology, Hyderabad, 500075, Telangana, India.
[d]Department of Sciences and Humanities, Matrusri Engineering College, Hyderabad, 500059, Telangana, India.
[e]Chemveda Life Sciences Pvt Ltd., IDA Uppal Hyderabad, 500039, Telangana, India.
**Corresponding author email: pochampalli.ou.chemi@gmail.com*

ABSTRACT:
A library of thirteen N-(4-(3-bromophenyl)thiazol-2-yl)-1-azaheteryl carboxamides were synthesized by a three component reaction of aminothiazole, various substituted piperazine or piperidines and triphosgene in presence of triethylamine. The structures of novel compounds were confirmed by ^{1}H-NMR, ^{13}C-NMR and LC-MS spectral techniques. The target compounds were screened for anticancer activity against breast cancer MCF-7 cell line by MTT assay. Most of the compounds showed promising cytotoxic activity with IC_{50} values in the range of 55 to 15 µg/mL and remaining molecules showed good to moderate activity compared to standard drug doxorubicin. The compounds substituted with 4-methyl piperidine, pyrrolidine and 4-isopropyl piperazine indicated promising activity against cancer cell lines. Molecular docking studies were performed against the crystal structures of Estrogen Receptor Alpha, Aurora-related kinase 1, 17β-Hydroxysteroid dehydrogenase and DNA topoisomerase 2-alpha using PyRx tool to validated the experimental results.

KEYWORDS: Urea, thiazole, breast cancer, MCF-7, molecular docking, PyRx

INTRODUCTION:

Urea derivatives are well-known organic compounds, that have attracted attention due to their diverse biological activities [i, ii]. These compounds are extensively used because of their virtuous pharmacological activities. The urea linkage is often present in various pharmacologically active drugs [iii, iv]. Diverse substitution at N-positions of urea derivatives generated a huge organic compounds, which exhibit wide range of applications, in particular, 1,3-disubstituted ureas with heterocyclic moiety as a substituent have gained medicinal importance. A prominent

class of heterocycles having a urea and a thiazole motif, notified as pharmacological agents and showing anticancer[v], anti-chronic myeloid leukemia[vi], anti-tuberculosis[vii], antibacterial[viii], antimalarial[ix], antiproliferative[x] and anti-inflammatory agents[xi].

In recent times, hybrid molecular systems with more nitrogen hetero atomic pharmacophores and two or more heterocyclic moieties having one to two hetero atoms, are exemplified for key leads or drugs in medicinal field. The 1,3-disubstituted urea with heterocyclic moiety at one of the nitrogen and other heterocycle by incorporation of second nitrogen forms the hybrid heterocycle with carboxamide linker. These carboxamide hybrid compounds are showing wide spread activities such as antibacterial[xii], myorelaxant[xiii], anticancer[xiv], antioxidant[xv], anticholinesterase[xvi], antiviral[xvii] and antiplasmodial activity[xviii], even some of them are marked drugs like sorafenib[xix-xxiv], larotrectinib[xxv, xxvi]. These are also emerged as interesting drug leads for cytotoxic activity as shown **Fig. 1**.

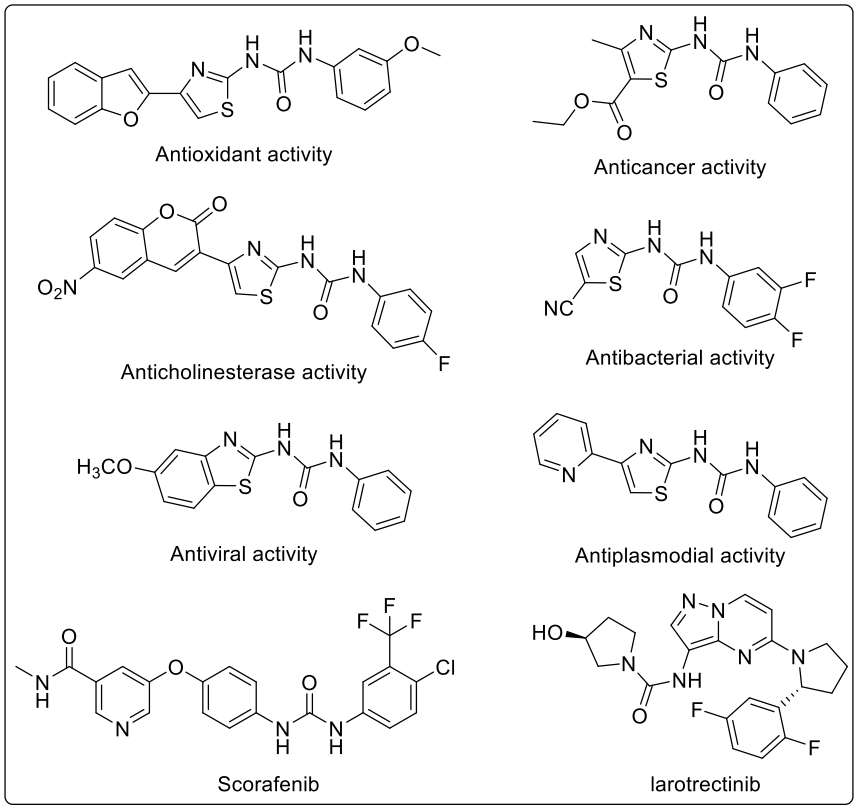

Fig-1: Representative examples of bioactive N-aryl-N'-2-thiazolylureas

2-Aminothiazole hybrids containing substituted urea were synthesized in various methods from 2-aminothiazole as precursor, and constructing a urea moiety on it using 4-nitrophenyl chloroformate[xxvii], 1,2-carbonyl diimidazole[xxviii], isocyanates[xxix, xxx], triphosgene[xxxi, xxxii] and carbon monoxide[xxxiii] reagents. The biological profiles of thiazole hybrids and in particular thiazole urea hybrids inspired us to develop a new series of bioactive thiazole-piperidine hybrids from 2-amino thiazole as key precursor. All the synthesized compounds were screened for cytotoxic activity against MCF-7 cancer cell lines. Molecular docking studies of the compounds was performed using Autodock Vina of PyRx[xxxiv, xxxv] on target proteins which are over expressed in cancer cells. The docking results showed the binding affinity of the protein-ligand complex and supports the cytotoxic activity results of the compounds.

EXPERIMENTAL SECTION

General Procedures

The ^{1}H NMR spectra were recorded on a Bruker AV 400 MHz instrument and the ^{13}C NMR spectra were recorded at 100 MHz using $CDCl_3$ as solvent. ESI-MS spectra was recorded on Agilent 1100 LC-Q TOF instrument. The melting point has determined in open capillaries and are uncorrected. Merck silica gel 60 F_{254} TLC plates were used.

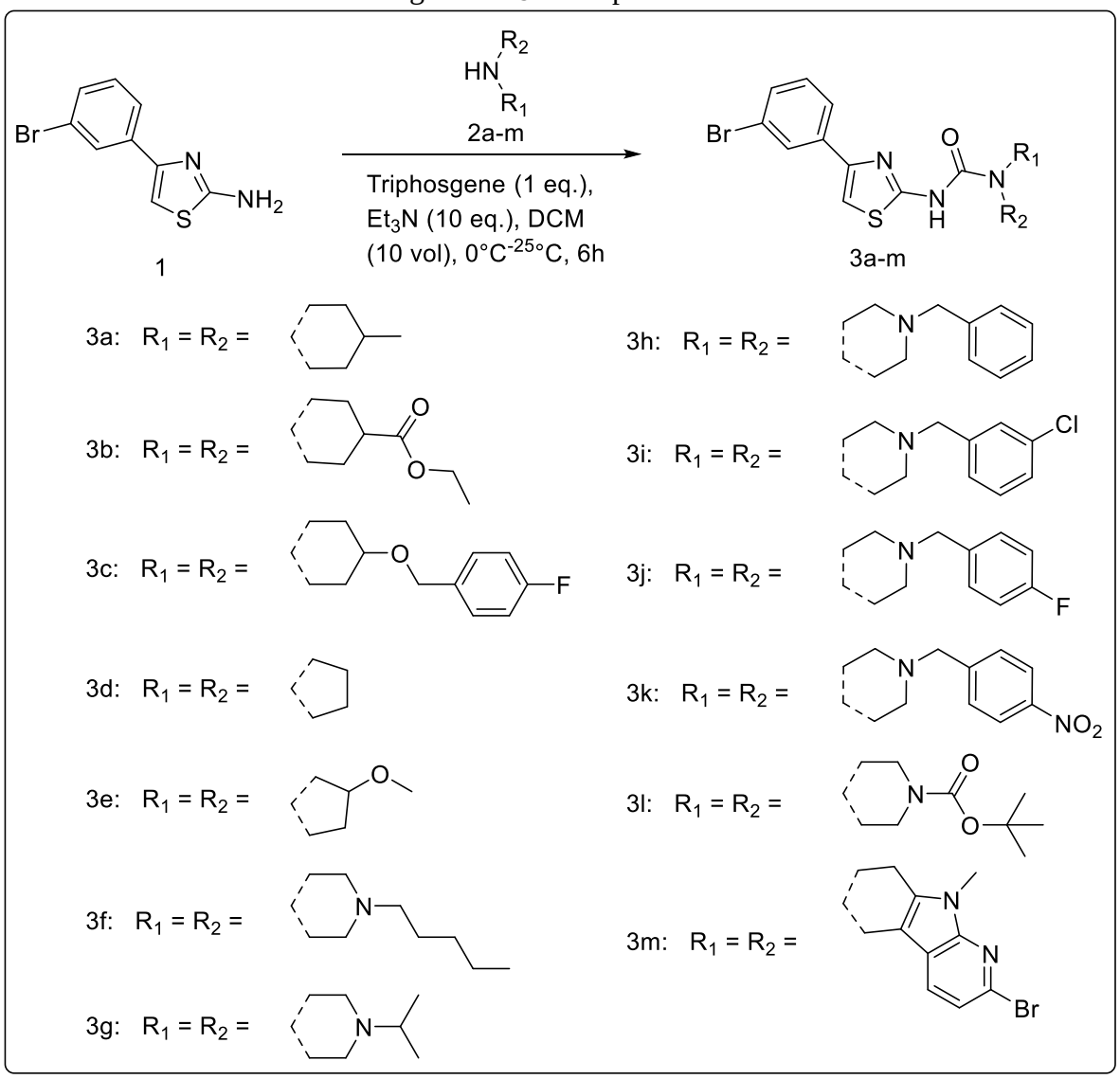

Scheme-1: Synthesis of thiazole-urea analogues **3(a-m)**

General procedure for the synthesis of N-(4-(3-bromophenyl)thiazol-2-yl)-1-azaheteryl carboxamides (3a-m): To a stirred solution of 4-(3-bromophenyl) thiazol-2-amine (**1**) (0.784 mmol, 1.0 eq.) in DCM (5 mL) was added triphosgene (0.784 mmol, 1.0 eq.) lot wise at 0 ˚C followed by addition of Et_3N (10.19 mmol, 13.0 eq.) drop wise. Then reaction mixture was stirred at 25 °C for 1 h. After 1h, was added compound (**2**) (1.175 mmol, 1.5 eq.) (dissolved in DCM (2 mL) at 0 °C. Reaction mixture was stirred at 0 °C for 6 h. After 6 h progress of the reaction monitored by TLC, polar spot was observed. Reaction mixture was diluted with DCM (10 mL) washed with water (10 mL) and sat. brine solution (10 mL). The organic layer was dried and concentrated to obtain crude product which further purified by silica gel column chromatography using 60-120 mesh gradient elution with 30% EtOAc/hexane to furnish the

corresponding 3-(4-(3-bromophenyl)thiazol-2-yl)-1- azaheteryl carboxamides **3(a-m**), presented in Scheme-1.

MTT Assay

The MCF-7 (Human Breast Cancer) cells, Dulbecco`s Modified Eagle Media (DMEM) with low glucose -Cat No-11965-092 (Gibco, Invitrogen), Fetal bovine serum (FBS) - Cat No - 10270106 (Gibco, Invitrogen), Antibiotic – Antimycotic 100X solution (Thermofisher Scientific)-Cat No-15240062 were purchased and used for MTT assay. The cells were seeded in a 96-well flat-bottom micro plate and maintained at 37ºC in 95% humidity and 5% CO_2 for overnight. Different concentration (50, 25, 12.50, 6.25 & 3.125 µg/ml) of samples were treated. The cells were incubated for another 48 hours. The wells were washed twice with PBS and 20 µL of the MTT staining solution was added to each well, and plate was incubated at 37ºC. After 4h, 100 µL of DMSO was added to each well to dissolve the formazan crystals, and absorbance was recorded with a 570 nm using micro plate reader[xxxvi]**.** The experiment was repeated three times, with the finding reported as mean ± SD.

Docking Protocol

PyRx docking protocol uses Autodock Vina[xxxvii] is an open source software installed into the computer configured with Intel(R) Core(TM) i5-8250U CPU @ 1.60GHz 1.80 GHz and 16 GB of RAM capacity. The crystal structures of Estrogen Receptor Alpha (ERα) (PDB ID: 3ERT)[xxxviii], Aurora-related kinase 1 (ARK) (PDB ID: 1MQ4) [xxxix], 17beta-hydroxysteroid dehydrogenase (17β-HSD1)[xl] (PDB ID:1FDW) and DNA topoisomerase 2-alpha (TOP2) (PDB ID: 5GWK) [xli] were retrieved from protein data bank. The active site pockets of target molecules were predicted by CASTp web server[xlii]. The ligands were sketched in MDL file format using Chemsketch tool and converted to PDB format using Pymol. Initially, the water molecules of receptor PDBs removed, polar hydrogens were added. Both macromolecule and ligands were loaded into PyRx tool. 3D grid box was set up to cover active site regions of receptor molecules with dimensions described in **Table-1** and docking simulations were performed by assigning exhaustiveness of 8. The results were ranked by considering lowest binding energy value of ligands as best confirmers. The binding interactions were visualized in Biovia Discovery Studio software tool.

Table-1: Dimensions of 3D grid box

Macromolecule	PDB ID	Grid coordinate (°A)
Estrogen Receptor Alpha	3ERT	center_x = 31.5126188761 center_y = -0.713918398076 center_z = 19.0584374698 size_x = 28.7907055458 size_y = 18.7963797091 size_z = 33.7124640221
Aurora-related kinase 1	1MQ4	center_x = -15.6782537072 center_y = 24.8508922287 center_z = 79.4213811887 size_x = 34.643289654 size_y = 26.4390853489 size_z = 23.3202376225
17β-Hydroxysteroid dehydrogenase	1FDW	center_x = 44.3764604597 center_y = -0.61629774727 center_z = 35.3731851434 size_x = 26.4083209194 size_y = 34.7096467118

		size_z = 37.4607634987
DNA topoisomerase II	5GWK	center_x = 15.7988259519 center_y = -43.7002699948 center_z = -55.1992776522 size_x = 41.9683213841 size_y = 25.1655546416 size_z = 26.6198576083

SPECTRAL DATA:

N-(4-(3-bromophenyl)thiazol-2-yl)-4-methylpiperidine-1-carboxamide (3a) as a white solid, yield: 76%, M.P. 90-92 °C. ^{1}H-NMR (400 MHz, $CDCl_3$) δ 8.45 br.s (1H), 7.96 t (*J*=1.6 Hz, 1H), 7.71-7.68 m (1H), 7.44-7.40 m (1H), 7.25 t (*J*=7.6 Hz, 1H), 7.06 s (1H), 4.05 d (*J*=12.8 Hz, 2H), 2.90 td (*J*=13.2, 2.8 Hz, 2H), 1.71 dd (*J*=13.2, 2.4 Hz, 2H), 1.66-1.54 m (1H), 1.21-1.10 m (2H), 0.96 d (*J*=6.8 Hz, 3H). ^{13}C NMR (100 MHz, $CDCl_3$) δ 161.18, 152.88, 147.98, 136.65, 130.64, 130.22, 129.06, 124.40, 122.93, 108.20, 44.53, 33.64, 30.69, 21.61. LC-MS purity: 98%, m/z 379.9 $[M+H]^+$.

Ethyl 1-((4-(3-bromophenyl)thiazol-2-yl)carbamoyl)piperidine-4-carboxylate (3b) as a pale-yellow solid, yield: 75%, M.P. 181-183 °C. ^{1}H-NMR (400 MHz, $CDCl_3$) δ 9.31 br.s (1H), 7.92 t (*J*=1.6 Hz, 1H), 7.66 dt (*J*=8.0, 1.2 Hz, 1H), 7.45-7.40 m (1H), 7.25 t (*J*=7.6 Hz, 1H), 7.08 s (1H), 4.14 q (*J*=14.4, 7.2 Hz, 2H), 3.93 d (*J*=13.2 Hz, 2H), 3.01-2.91 m (2H), 2.49-2.42 m (1H), 1.93-1.85 m (2H), 1.68-1.55 m (2H), 1.25 t (*J*=6.8 Hz, 3H). ^{13}C NMR (100 MHz, $CDCl_3$) δ 173.88, 161.58, 153.14, 147.91, 136.49, 130.73, 130.28, 129.08, 124.43, 122.97, 108.43, 60.72, 43.45, 40.49, 27.55, 14.20. LC-MS purity: 98%, m/z 439.9 $[M+H]^+$.

N-(4-(3-bromophenyl)thiazol-2-yl)-4-((4-fluorobenzyl)oxy)piperidine-1-carboxamide (3c) as a pale-yellow solid, yield: 76%, M.P. 131-133 °C. ^{1}H-NMR (400 MHz, $CDCl_3$) δ 8.52 br.s (1H), 7.95 t (*J*=1.6 Hz, 1H), 7.69 dt (*J*=8.0, 1.2 Hz, 1H), 7.44-7.40 m (1H), 7.33-7.28 m (2H), 7.26 t (*J*=7.6 Hz, 1H), 7.07 s (1H), 7.04 t (*J*=8.4 Hz, 2H), 4.52 s (2H), 3,78-3.69 m (2H), 3.69-3.63 m (1H), 3.40-3.32 m (2H), 1.93-1.84 m (2H), 1.76-1.67 m (2H). ^{13}C NMR (100 MHz, $CDCl_3$) δ 163.36, 161.40, 160.92, 153.15, 147.93, 136.52, 133.22, 133.20, 130.76, 130.57, 130.49, 130.31, 129.11, 124.45, 122.99, 115.30, 115.09, 108.44, 61.97, 52.22, 43.99. LC-MS purity: 95%, m/z 490.0 $[M+H]^+$.

N-(4-(3-bromophenyl)thiazol-2-yl)pyrrolidine-1-carboxamide (3d) as a pale-yellow solid, yield: 80%, M.P. 80-82 °C. ^{1}H-NMR (400 MHz, $CDCl_3$) δ 8.36 br.s (1H), 7.95 t (*J*=1.6 Hz, 1H), 7.69 dt (*J*=8.0, 1.2 Hz, 1H), 7.44-7.40 m (1H), 7.25 t (*J*=7.6 Hz, 1H), 7.05 s (1H), 3.47 br.s (4H), 1.96 br.s (4H). ^{13}C NMR (100 MHz, $CDCl_3$) δ 160.52, 152.07, 147.91, 136.63, 130.64, 130.21, 129.00, 124.41, 122.89, 108.07, 45.89, 25.51. LC-MS purity: 98%, m/z 353.9 $[M+H+2]^+$.

N-(4-(3-bromophenyl)thiazol-2-yl)-3-methoxypyrrolidine-1-carboxamide (3e) as a pale-yellow semisolid, yield: 78%, ^{1}H-NMR (400 MHz, $CDCl_3$) δ 8.79 br.s (1H), 7.93 t (*J*=1.6 Hz, 1H), 7.67 d (*J*=8.0 Hz, 1H), 7.44-7.40 m (1H), 7.25 t (*J*=7.6 Hz, 1H), 7.04 s (1H), 3.59-3.49 m (3H), 3.32 s (3H), 2.19-2.07 m (2H), 2.06-1.93 m (2H). ^{13}C NMR (100 MHz, $CDCl_3$) δ 160.52, 152.07, 147.91, 136.63, 130.64, 130.21, 129.00, 124.41, 122.89, 108.07, 45.89, 25.51. LC-MS purity: 90%, m/z 383.9 $[M+H]^+$.

N-(4-(3-bromophenyl)thiazol-2-yl)-4-pentylpiperazine-1-carboxamide (3f) as a white solid, yield: 71%, M.P. 84-86 °C. ^{1}H-NMR (400 MHz, $CDCl_3$) δ 7.93 t (*J*=1.6 Hz, 1H), 7.67 dt (*J*=7.6, 1.2 Hz, 1H), 7.45-7.40 m (1H), 7.26 t (*J*=8.0 Hz, 1H), 7.06 s (1H), 3.54 t (*J*=4.8, 4H), 2.45 t (*J*=4.8 Hz, 4H), 2.34 t (*J*=8.0 Hz, 2H), 1.54-1.45 m (2H), 1.37-1.24 m (4H), 0.90 t (*J*=6.8 Hz, 3H). ^{13}C NMR (100 MHz, $CDCl_3$) δ 160.93, 152.91, 147.99, 136.53, 130.73,

130.26, 129.06, 124.39, 122.97, 108.31, 58.53, 52.55, 43.98, 29.65, 26.43, 22.59, 14.04. LC-MS purity: 99%, m/z 439.0 $[M+H]^{+}$.

N-(4-(3-bromophenyl) thiazol-2-yl)-4-isopropylpiperazine-1-carboxamide (3g) as a light brown solid, yield: 72%, M.P. 120-122 °C. ^{1}H-NMR (400 MHz, $CDCl_3$) δ 7.90 s 1(H), 7.65 d (*J*=7.6 Hz, 1H), 7.44-7.40 m (1H), 7.25 t (*J*=8.0 Hz, 1H), 7.08 s (1H), 3.45 s (4H), 2.71-2.62 m (1H), 2.39 s (4H), 0.99 d (*J*=6.4 Hz, 6H). ^{13}C-NMR (100 MHz, $CDCl_3$) δ 161.81, 153.22, 147.85, 136.43, 130.77, 130.34, 129.10, 124.46, 123.03, 108.44, 54.49, 47.91, 44.28, 18.26. LC-MS purity: 97.8%, m/z 408.9 $[M+H]^{+}$.

4-benzyl-N-(4-(3-bromophenyl)thiazol-2-yl)piperazine-1-carboxamide (3h) as a pale-yellow solid, yield: 69%, M.P. 122-124 °C. ^{1}H-NMR (400 MHz, $CDCl_3$) δ 9.47 br.s (1H), 7.91 t (*J*=1.6 Hz, 1H), 7.66-7.63 m (1H), 7.45-7.40 m (1H), 7.34-7.22 m (6H), 7.07 s (1H), 3.45 s (2H), 3.42 t (*J*=4.8, 4H), 2.32 t (*J*=4.8 Hz, 4H). ^{13}C NMR (100 MHz, $CDCl_3$) δ 161.42, 153.17, 147.93, 137.50, 136.54, 130.74, 130.31, 129.10, 128.37, 127.34, 124.45, 123.00, 108.42, 62.81, 52.31, 44.02. LC-MS purity: 98%, m/z 458.9 $[M+H]^{+}$.

N-(4-(3-bromophenyl)thiazol-2-yl)-4-(3-chlorobenzyl)piperazine-1-carboxamide (3i) as a light brown solid., yield: 70%, M.P. 82-84 °C. ^{1}H-NMR (400 MHz, $CDCl_3$) δ 9.28 br.s (1H), 7.91 t (*J*=2.0 Hz, 1H), 7.65 d (*J*=8.0 Hz, 1H), 7.45-7.41 m (1H), 7.31 s (1H), 7.28-7.22 m (3H), 7.19-7.14 m (1H), 7.08 s (1H), 3.45 t (*J*=4.4 Hz, 4H), 3.43 s (2H), 2.33 t (*J*=4.4 Hz, 4H). ^{13}C NMR (100 MHz, $CDCl_3$) δ 161.84, 153.33, 153.21, 147.85, 139.75, 136.49, 134.29, 130.78, 130.37, 129.63, 129.15, 128.96, 127.52, 127.09, 124.49, 123.02, 108.52, 62.13, 52.22, 43.95. LC-MS purity: 99.4%, m/z 492.9 $[M+H]^{+}$.

N-(4-(3-bromophenyl)thiazol-2-yl)-4-(4-fluorobenzyl)piperazine-1-carboxamide (3j) as a pale yellow solid, yield: 68%, M.P. 87-89 °C. ^{1}H-NMR (400 MHz, $CDCl_3$) δ 9.32 br.s (1H), 7.90 t (*J*=2.0 Hz, 1H), 7.65 d (*J*=8.0 Hz, 1H), 7.45-7.41 m (1H), 7.28-7.22 m (3H), 7.07 s (1H), 7.04-6.97 m (2H), 3.43 t (*J*=4.4 Hz, 4H), 3.42 s (2H), 2.32 t (*J*=4.4 Hz, 4H). ^{13}C NMR (100 MHz, $CDCl_3$) δ 163.35, 161.28, 160.92, 153.08, 147.92, 136.49, 133.15, 130.76, 130.59, 130.51, 130.31, 129.09, 124.44, 122.98, 115.31, 115.10, 108.41, 61.97, 52.22, 43.96. LC-MS purity: 99.4%, m/z 477.0 $[M+H+2]^{+}$.

N-(4-(3-bromophenyl)thiazol-2-yl)-4-(4-nitrobenzyl)piperazine-1-carboxamide (3k) as a light brown solid, yield: 70%, M.P. 85-87 °C. ^{1}H-NMR (400 MHz, $CDCl_3$) δ 9.32 br.s (1H), 8.19 dt (*J*=8.8 Hz, 2H), 7.91 t (*J*=2.0 Hz, 1H), 7.66 dt (*J*=8.0 Hz, 1H), 7.49 d (*J*=8.8 Hz, 2H), 7.46-7.42 m (1H), 7.26 t (*J*=8.0 Hz, 1H), 7.09 s (1H), 3.55 s (2H), 3.46 t (*J*=4.8, 4H), 2.35 t (*J*=4.8 Hz, 4H). ^{13}C NMR (100 MHz, $CDCl_3$) δ 161.38, 153.15, 147.91, 147.36, 145.48, 136.48, 130.80, 130.35, 129.45, 129.11, 124.46, 123.68, 123.00, 108.49, 61.88, 52.40, 43.94. LC-MS purity: 93.05%, m/z 502.0 $[M+-H]^{+}$.

Tert-butyl 4-(4-(3-bromophenyl) thiazol-2-ylcarbamoyl)piperazine-1-carboxylate (3l) as a pale-yellow solid, yield: 78%, M.P. 176-178 °C. ^{1}H-NMR (400 MHz, $CDCl_3$) δ 9.48 br.s (1H), 7.91 t (*J*=2.0 Hz, 1H), 7.65 dt (*J*=7.6, 1.6 Hz, 1H), 7.44-7.41 m (1H), 7.25 t (*J*=8.0 Hz, 1H), 7.10 s (1H), 3.43-3.38 m (4H), 3.38-3.33 m (4H), 1.45 s (9H). ^{13}C NMR (100 MHz, $CDCl_3$) δ 161.42, 154.45, 153.37, 147.87, 136.33, 130.84, 130.33, 129.09, 124.42, 123.01, 108.58, 80.50, 43.71, 28.37. LC-MS purity: 98.6%, m/z 465.0 $[M-H]^{-}$.

2-bromo-N-(4-(3-bromophenyl)thiazol-2-yl)-9-methyl-5,7,8,9-tetrahydro-6H-pyrrolo[2,3-b:4,5-c']dipyridine-6-carboxamide (3m) as a yellow solid, yield: 65%, M.P. 151-153 °C. ^{1}H-NMR (400 MHz, $CDCl_3$) δ 10.07 br.s (1H), 7.72 t (*J*=1.6 Hz, 1H), 7.41 dt (*J*=8.0, 1.2 Hz, 1H), 7.34-7.29 m (2H), 7.14 d (*J*=8.0 Hz, 1H), 7.11 t (*J*=7.6 Hz, 1H), 7.03 s (1H), 4.56 s (2H), 3.93 t (*J*=5.6 Hz, 2H), 3.65 s (3H), 2.76 t (*J*=5.6 Hz, 2H). ^{13}C NMR (100 MHz, $CDCl_3$) δ 161.68, 153.66, 147.86, 147.61, 136.06, 134.43, 133.95, 130.46, 130.02, 128.81, 127.22, 124.10, 122.76, 118.85, 116.09, 108.58, 103.76, 41.40, 40.94, 28.06, 22.09. LC-MS purity: 91%, m/z 547.8 $[M+H]^{+}$.

RESULTS AND DISCUSSION:

Chemistry

The synthesis of the titled hybrid compounds having thiazole and saturated aza heterocycle scaffolds with carboxamide linker was taken up from the base catalysed three component reaction in a simple, single step using 2-aminothiazole **1** and aza heterocycle with free NH as suitable precursors. Triphosgene was used as carbonyl source. As representative example, the reaction of amino compound **1**, 4-methylpiperidine **2a** with free NH group and triphosgene was carried out using triethyl amine as base at 0 °C in DCM for 6 h. After usual work up followed by purification of the crude product using column chromatography yielded the target hybrid disubstituted carboxamide derivative **3a** in 76% yield (Scheme-1).The compound **3a** showed the prominent peaks like broad singlet at δ 8.45 for carboxamide N<u>H</u>, a singlet at δ 7.6 for thiazole ring proton, and two peaks at δ 4.05 as broad doublet, 2.90 as doublet of triplet for piperidine ring nitrogen attached four C<u>H</u>$_2$ protons, and remaining ring five protons gives signals at δ 1.71 as broad doublet for two protons, δ 1.66-1.54 as multiplet for one proton and δ 1.21 – 1.09 as multiplet for two protons and δ 0.96 as doublet for three methyl protons in 1H NMR spectrum. The product also showed the amide carbonyl carbon peak at δ 161.18, the presence of 4-methyl piperidine ring is also confirmed by the presence of δ 44.53, 33.64, 30.69, 21.61 in ^{13}C NMR spectrum. Further the structure for the product **3a** is confirmed by the presence of protonated molecular ion peak at m/z 379.9 $[M+H]^+$ in its mass spectrum. The novel carboxamide series **3(b-e)** were isolated in a one-step reaction of aminothiazole **1**, triphosgene and aza heterocycle **2(b-e)**. Two piperidine derivatives **2b**, **2c** and two pyrrolidines **2d** and **2e** were used as aza heterocycles with free NH group. Using piperazine derivatives **2(f-l)** and fused piperazine analogue **2m**, another carboxamide hybrids with diaza heterocycle derivative / fused piperidine heterocycle **3(f-m)** were prepared (Scheme-1) and all these compounds were confirmed based on their analytical techniques and are given in experimental section.

Anticancer Activity

The synthesised targets **3(a-m)** were screened for cytotoxic activity against MCF-7 cell lines at various concentrations 50, 25, 12.50, 6.25, 3.125 µM. The test results for cell viability and IC_{50} values were presented in Table-2. DMSO solvent was used as blank control and *Doxorubicin* was used as standard and its IC_{50} value is indicated as 7.54 µM, and in comparison with it, all compounds exhibited anticancer activity against MCF-7 cell lines except **3c, 3f, 3i, 3k** and **3m**. Compounds **3b**, **3e**, **3h**, **3j** and **3l** showed moderate activity in the range of IC_{50} values 55-28 µM concentration and the other compounds such as **3a**, **3d** and **3g** possess high activity with IC_{50} values 17.5, 14.05 and 20.94 µM.

Table-2: The Cell viability and IC_{50} values of compounds 3(a-m) against MCF-7 cell line

Compound	Cell viability					IC_{50}
	Concentration					
	50	25	12.5	6.25	3.125	
3a	42.65	44.55	52.13	55.45	68.25	17.54
3b	54.98	55.92	70.14	87.68	96.21	55.24
3c	72.04	75.36	76.78	84.36	85.78	132.77
3d	45.02	45.97	49.76	64.45	75.36	14.05

3e	32.23	65.88	66.82	82.94	86.26	33.93
3f	64.45	66.82	75.36	82.94	83.36	80.68
3g	30.33	36.97	58.29	78.67	88.15	20.94
3h	47.87	62.09	72.99	74.41	76.78	41.10
3i	71.56	74.88	78.20	82.94	91.47	123.73
3j	56.40	57.35	65.88	74.88	78.67	48.25
3k	72.51	78.20	80.57	91.94	97.63	150.27
3l	42.65	45.97	56.40	73.93	85.78	22.65
3m	71.09	73.46	74.88	85.78	88.15	107.10
Doxorubicin	35.69	38.24	41.64	43.34	49.01	7.54

Molecular Docking Studies

To validate the activity of novel compounds, molecular docking studies were performed against the crystal structures of Estrogen Receptor Alpha (ERα) (PDB ID: 3ERT), Aurora-related kinase 1 (ARK) (PDB ID: 1MQ4), 17beta-hydroxysteroid dehydrogenase (17β-HSD1) (PDB ID:1FDW) and DNA topoisomerase 2-alpha (TOP2) (PDB ID: 5GWK). ERα plays an important role in mammary gland biology and breast cancer progression[xliii-xlv]. Aurora kinases promote cell cycle and survival of cancer cells [xlvi, xlvii]. 17β-HSD1 is responsible for the production of estrogens estradiol and 5-androsten-3β,17β-diol consequently it is a target of choice for the treatment of estrogen-dependent diseases such as breast cancer and endometriosis, by blocking estrogen biosynthesis [xlviii]. Inhibition of DNA topoisomerase II cause cancer cell death by inducing DNA damage [xlix, l]. That is the reason we have chosen these targets for molecular docking study. All compounds along with standard reference doxorubicin were docked into the active site pockets of target PDBs and binding energies are tabulated in **Table-3**.

Table-3: Binding affinities of compounds **3(a-m)** against cancer drug targets

Compound	Binding Energy Kcal/mol			
	3ERT	1MQ4	1FDW	5GWK
3a	-7.9	-8.8	-7.6	-7.9
3b	-7.8	-8.9	-7.9	-7.1
3c	-9.4	-10.3	-8.9	-8.7
3d	-7.4	-8.4	-7.1	-7.9
3e	-7.2	-8.3	-7.3	-7.1
3f	-7.7	-8.7	-7.5	-7.4
3g	-7.6	-8.8	-7.9	-7.7
3h	-9.2	-9.9	-8.5	-8.4
3i	-9.0	-10.0	-8.8	-8.5
3j	-9.2	-9.8	-8.8	-8.4
3k	-8.8	-10.2	-9.4	-8.1
3l	-7.9	-9.0	-8.4	-7.5
3m	-9.3	-11.0	-9.1	-8.6
Doxorubicin	-8.2	-9.8	-8.4	-8.3

Compounds **3c, 3h, 3i, 3j, 3k** and **3m** scored best binding affinity values against ERα (PDB ID: 3ERT) with reference to *Doxorubicin*. Among which **3c** indicated highest docking score of -9.4 Kcal/mol, it indicated a key interaction with Arg394 and hydrophobic interactions

with Leu346, Thr347, Ala350, Glu353, Leu387, Leu391, Leu525, Lys529, Cys530, Val533 of ERα, shown in **Fig 2**. Whereas *Doxorubicin* scored binding affinity value of -8.2 Kcal/mol against the ERα, by demonstrating H-bond interactions against Glu380, Cys530, Val534, Leu536 and hydrophobic interactions with Ala350, Asp351, Trp383, Met522, Cys530, Val534, Pro535, Leu536 in active site pocket of ERα (**Fig 3**). Similarly, the same compounds **3c, 3h, 3i, 3j, 3k** and **3m** specified best binding affinity against ARK (PDB ID: 1MQ4) compared to *Doxorubicin*. Compound **3m** possesses highest binding energy value of -11.0 Kcal/mol against ARK by establishing H-bond interactions with Lys143, Lys162, Asp274 which are essential in predicting activity (**Fig 4**). And *Doxorubicin* demonstrated H-bond interactions with Lys143, Glu260, Asn261, Asn274 with a binding energy value of -9.8 Kcal/mol against ARK (**Fig 5**). Against 17β-HSD1 (PDB ID: 1FDW), the docking scores of compounds **3c, 3h, 3l, 3i, 3j, 3k** and **3m** are comparable to *Doxorubicin*. Highest binding affinity was scored by compound **3k** with a value of -9.4 Kcal/mol and doxorubicin scored -8.4 Kcal/mol. The docking pose and interactions of compound **3k** and *Doxorubicin* with 17β-HSD1, are represented in **Fig 6** and **Fig 7** respectively. Compounds **3c, 3h, 3j, 3k** and **3m** binding affinities against TOP2 (PDB ID: 5GWK) are notably good than *Doxorubicin*. Compound **3c** scored higher value of -8.7 Kcal/mol whereas doxorubicin scored -8.3 Kcal/mol. The binding interactions of **3c** and *Doxorubicin* with TOP2 are demonstrated in **Fig 8** and **Fig 9** respectively.

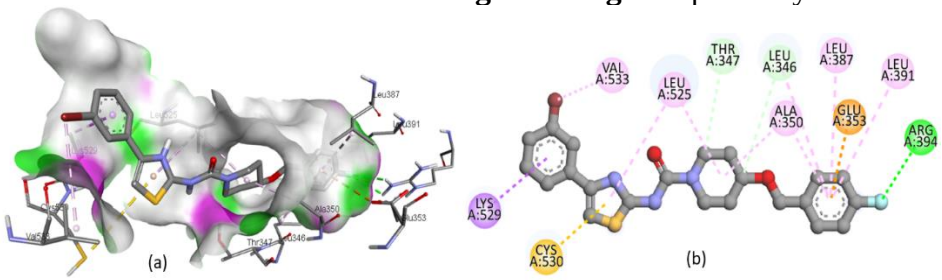

Fig 2. (a) Docking pose and (b) 2D interactions of compound **3c** in cavity of ERα

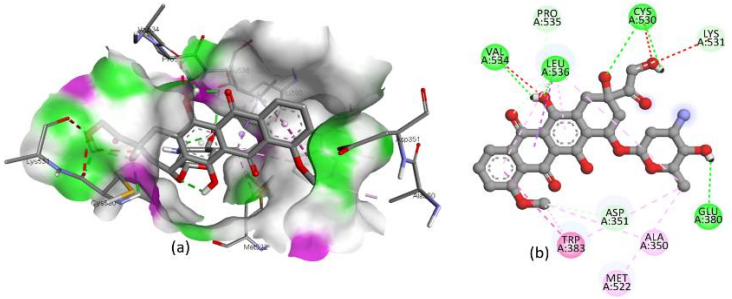

Fig 3. (a) Docking pose and (b) 2D interactions of *Doxorubicin* in cavity of ERα

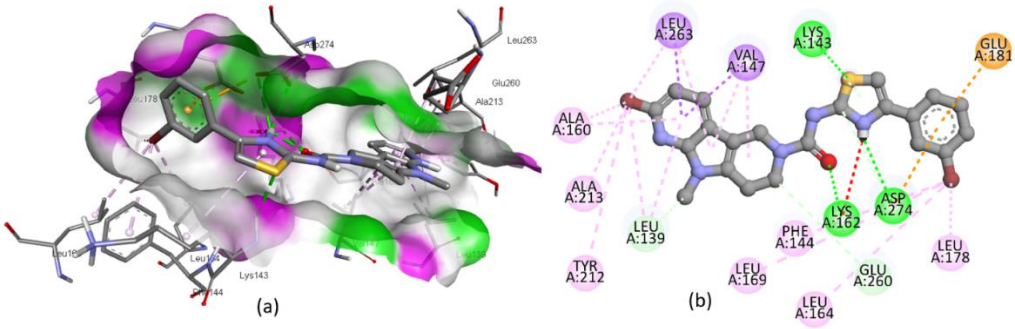

Fig 4. (a) Docking pose and (b) 2D interactions of compound **3m** in cavity of Aurora kinase

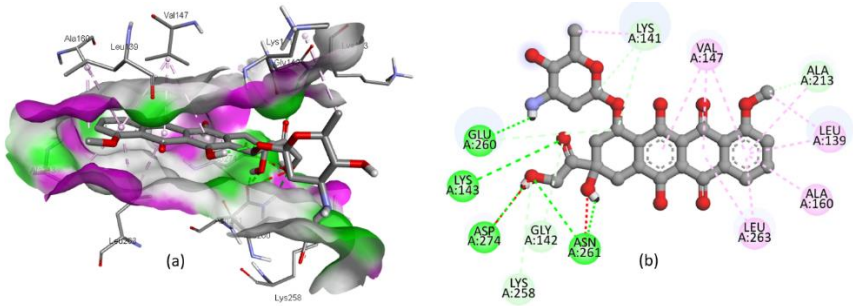

Fig 5. (a) Docking pose and (b) 2D interactions of *Doxorubicin* in cavity of Aurora kinase

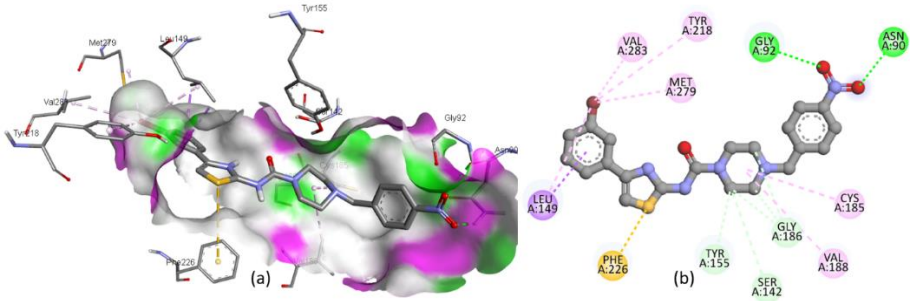

Fig 6. (a) Docking pose and (b) 2D interactions of compound **3k** in cavity of 17β-HSD1

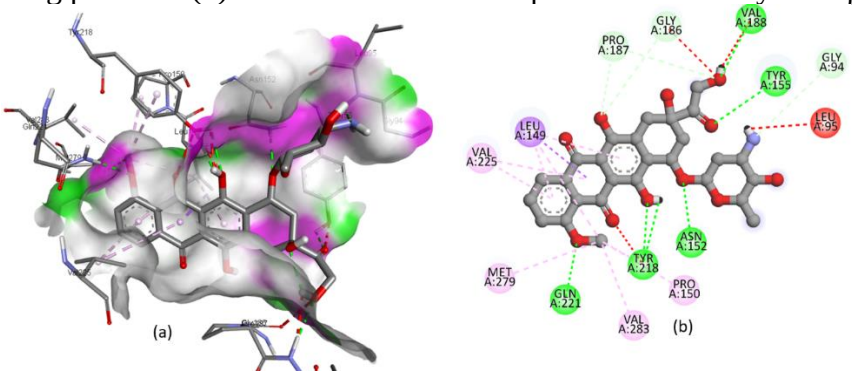

Fig 7. (a) Docking pose and (b) 2D interactions of *Doxorubicin* in cavity of 17β-HSD1

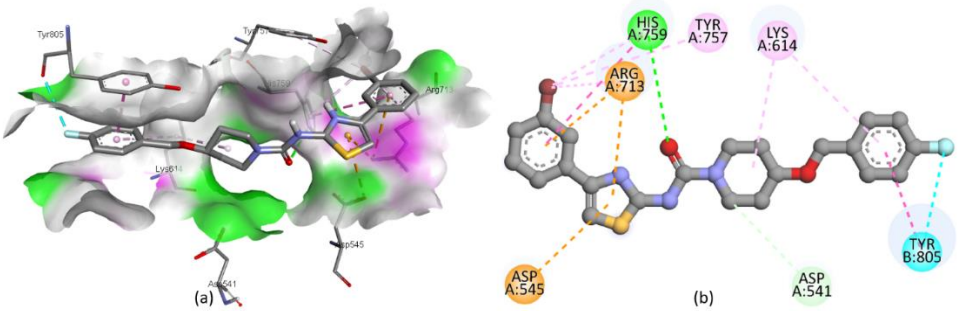

Fig 8. (a) Docking pose and (b) 2D interactions of compound **3c** in cavity of DNA Topoisomerase II.

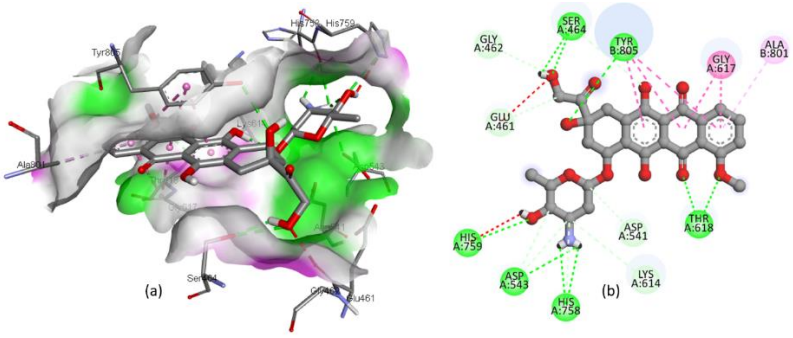

Fig 9. (a) Docking pose and (b) 2D interactions of *Doxorubicin* in cavity of DNA Topoisomerase II.

CONCLUSION

A new series of thiazole based carboxamide hybrid compounds were synthesized in a base catalysed one pot three component reaction from thiazole-based amine, aza heterocycle with free NH group. Pyrrolidine, piperidine and piperazines were used as aza heterocycles. All the hybrid compounds are characterized using spectral techniques and those are screened for cytotoxicity against MCF-7 cancer cell lines. The activity results indicated the moderate to good anti proliferation of most of the compounds. **3a**, **3d** and **3g** possess high activity with IC_{50} values 17.5, 14.05 and 20.94 µM. The molecular docking studies investigations are in support of experimental evidence.

ACKNOWLEDGEMENTS

I am thankful to Jawaharlal Nehru Technological University for providing research opportunity. I thank Chemveda Life Sciences for providing laboratory facilities.

REFERENCES

i M. Patil, A.N. Poyil, S.D. Joshi, S.A. Patil, S.A. Patil, A. Bugarin, Synthesis, molecular docking studies, and antimicrobial evaluation of new structurally diverse ureas, Bioorg Chem.; 2019, **87**, 302–311.

ii S.A. Khan, N. Singh, K. Saleem, Synthesis, characterization and in vitro antibacterial activity of thiourea and urea derivatives of steroids, Eur J Med Chem.; 2008, **43** (10)**,** 2272–2277.

iii N. Kapuriya, K. Kapuriya, X. Zhang, T.-C. Chou, R. Kakadiya, Y.-T. Wu, T.-H. Tsai, Y.-T. Chen, T.-C. Lee, A. Shah, Synthesis and biological activity of stable and potent antitumor agents, aniline nitrogen mustards linked to 9-anilinoacridines via a urea linkage, Bioorg Med Chem.; 2008, **16** (10), 5413–5423.

iv P.C. Singh, S.K. Ballas, Emerging drugs for sickle cell anemia, Expert Opin Emerg Drugs.; 2015, **20** (1), 47–61.

v N. Selvakumaran, N.S.P. Bhuvanesh, A. Endo, R. Karvembu, Synthesis, structure, DNA and protein binding studies, and cytotoxic activity of nickel (II) complexes containing 3, 3-dialkyl/aryl-1-(2, 4-dichlorobenzoyl) thiourea ligands, Polyhedron.; 2014, **75**, 95–109.

vi W. Li, J. Chu, T. Fan, W. Zhang, M. Yao, Z. Ning, M. Wang, J. Sun, X. Zhao, A. Wen, Design and synthesis of novel 1-phenyl-3-(5-(pyrimidin-4-ylthio)-1, 3, 4-thiadiazol-2-yl) urea derivatives with potent anti-CML activity throughout PI3K/AKT signaling pathway, Bioorg Med Chem Lett.; 2019, **29** (14), 1831–1835.

vii R.S. Upadhayaya, G.M. Kulkarni, N.R. Vasireddy, J.K. Vandavasi, S.S. Dixit, V. Sharma, J. Chattopadhyaya, Design, synthesis and biological evaluation of novel triazole, urea and thiourea derivatives of quinoline against Mycobacterium tuberculosis, Bioorg Med Chem.; 2009, **17** (13) 4681–4692.

viii M. Gemili, H. Sari, M. Ulger, E. Sahin, Y. Nural, Pt (II) and Ni (II) complexes of octahydropyrrolo [3, 4-c] pyrrole N-benzoylthiourea derivatives: synthesis, characterization, physical parameters and biological activity, Inorganica Chim Acta.; 2017, **463**, 88–96.

ix T.J. Egan, K.R. Koch, P.L. Swan, C. Clarkson, D.A. van Schalkwyk, P.J. Smith, In vitro antimalarial activity of a series of cationic 2, 2 '-Bipyridyl-and 1, 10-Phenanthrolineplatinum (II) benzoylthiourea complexes, J Med Chem.; 2004, **47** (11), 2926–2934.

x T.M. Wrobel, M. Kiełbus, A.A. Kaczor, V. Kryštof, Z. Karczmarzyk, W. Wysocki, A. Fruziński, S.K. Król, A. Grabarska, A. Stepulak, Discovery of nitroaryl urea derivatives with antiproliferative properties, J Enzyme Inhib Med Chem.; 2016, **31** (4), 608–618.

xi R.H. Tale, A.H. Rodge, G.D. Hatnapure, A.P. Keche, The novel 3, 4-dihydropyrimidin-2 (1H)-one urea derivatives of N-aryl urea: synthesis, anti-inflammatory, antibacterial and antifungal activity evaluation, Bioorg Med Chem Lett.; 2011, **21** (15), 4648–4651.

xii G.D. Francisco, Z. Li, J.D. Albright, N.H. Eudy, A.H. Katz, P.J. Petersen, P. Labthavikul, G. Singh, Y. Yang, B.A. Rasmussen, Phenyl thiazolyl urea and carbamate derivatives as new inhibitors of bacterial cell-wall biosynthesis, Bioorg Med Chem Lett.; 2004, **14** (1), 235–238.

xiii K. Harrouche, J.-F. Renard, N. Bouider, P. de Tullio, E. Goffin, P. Lebrun, G. Faury, B. Pirotte, S. Khelili, Synthesis, characterization and biological evaluation of benzothiazoles and tetrahydrobenzothiazoles bearing urea or thiourea moieties as vasorelaxants and inhibitors of the insulin releasing process, Eur J Med Chem.; 2016, **115,** 352–360.

xiv S.A.F. Rostom, H.M. Faidallah, M.F. Radwan, M.H. Badr, Bifunctional ethyl 2-amino-4-methylthiazole-5-carboxylate derivatives: Synthesis and in vitro biological evaluation as antimicrobial and anticancer agents, Eur J Med Chem.; 2014, **76,** 170–181.

xv B.Z. Kurt, I. Gazioglu, L. Basile, F. Sonmez, T. Ginex, M. Kucukislamoglu, S. Guccione, Potential of aryl–urea–benzofuranylthiazoles hybrids as multitasking agents in Alzheimer's disease, Eur J Med Chem.; 2015, **102**, 80–92.

xvi B.Z. Kurt, I. Gazioglu, F. Sonmez, M. Kucukislamoglu, Synthesis, antioxidant and anticholinesterase activities of novel coumarylthiazole derivatives, Bioorg Chem.; 2015, **59**, 80–90.

xvii Y. Xie, S. Deng, Z. Chen, S. Yan, D.W. Landry, Identification of small-molecule inhibitors of the Aβ–ABAD interaction, Bioorg Med Chem Lett.; 2006, **16** (17), 4657–4660.

xviii F. Mjambili, M. Njoroge, K. Naran, C. de Kock, P.J. Smith, V. Mizrahi, D. Warner, K. Chibale, Synthesis and biological evaluation of 2-aminothiazole derivatives as antimycobacterial and antiplasmodial agents, Bioorg Med Chem Lett.; 2014, **24** (2), 560–564.

xix S. Sun, Z. He, M. Huang, N. Wang, Z. He, X. Kong, J. Yao, Design and discovery of thioether and nicotinamide containing sorafenib analogues as multikinase

inhibitors targeting B-Raf, B-RafV600E and VEGFR-2, Bioorg Med Chem.; 2018, **26** (9), 2381–2391.

xx S. Zhou, G. Chen, Design, synthesis, and bioactivity evaluation of antitumor sorafenib analogues, RSC Adv.; 2018, **8** (66), 37643–37651.

xxi W. Wang, C. Wu, J. Wang, R. Luo, C. Wang, X. Liu, J. Li, W. Zhu, P. Zheng, Synthesis, activity and docking studies of phenylpyrimidine–carboxamide Sorafenib derivatives, Bioorg Med Chem.; 2016, **24** (23), 6166–6173.

xxii M. Wang, S. Xu, H. Lei, C. Wang, Z. Xiao, S. Jia, J. Zhi, P. Zheng, W. Zhu, Design, synthesis and antitumor activity of Novel Sorafenib derivatives bearing pyrazole scaffold, Bioorg Med Chem.; 2017, **25** (20), 5754–5763.

xxiii W. Zhan, Y. Li, W. Huang, Y. Zhao, Z. Yao, S. Yu, S. Yuan, F. Jiang, S. Yao, S. Li, Design, synthesis and antitumor activities of novel bis-aryl ureas derivatives as Raf kinase inhibitors, Bioorg Med Chem.; 2012, **20** (14), 4323–4329.

xxiv J. Yao, J. Chen, Z. He, W. Sun, W. Xu, Design, synthesis and biological activities of thiourea containing sorafenib analogs as antitumor agents, Bioorg Med Chem.; 2012, **20** (9), 2923–2929.

xxv A. Drilon, T.W. Laetsch, S. Kummar, S.G. DuBois, U.N. Lassen, G.D. Demetri, M. Nathenson, R.C. Doebele, A.F. Farago, A.S. Pappo, Efficacy of larotrectinib in TRK fusion–positive cancers in adults and children, New England Journal of Medicine.; 2018, **378** (8), 731–739.

xxvi N. Federman, C.M. Albert, B. Turpin, L. Mascarenhas, R. Nagasubramanian, B. Geoerger, M. Casanova, M.S. Gallego Melcon, J. Chisholm, C.M. van Tilburg, Phase 1/2 study of the selective TRK inhibitor larotrectinib in pediatric patients with cancer.; 2017, TPS10577-TPS10577.

xxvii A. Abibi, A.D. Ferguson, P.R. Fleming, N. Gao, L.I. Hajec, J. Hu, V.A. Laganas, D.C. McKinney, S.M. McLeod, D.B. Prince, The role of a novel auxiliary pocket in bacterial phenylalanyl-tRNA synthetase druggability, Journal of Biological Chemistry.; 2014, **289** (31), 21651–21662.

xxviii Y. Xie, S. Deng, Z. Chen, S. Yan, D.W. Landry, Identification of small-molecule inhibitors of the Aβ–ABAD interaction, Bioorg Med Chem Lett.; 2006, **16** (17), 4657–4660.

xxix K. Harrouche, J.-F. Renard, N. Bouider, P. de Tullio, E. Goffin, P. Lebrun, G. Faury, B. Pirotte, S. Khelili, Synthesis, characterization and biological evaluation of benzothiazoles and tetrahydrobenzothiazoles bearing urea or thiourea moieties as vasorelaxants and inhibitors of the insulin releasing process, Eur J Med Chem.; 2016, **115,** 352–360.

xxx F. Mjambili, M. Njoroge, K. Naran, C. de Kock, P.J. Smith, V. Mizrahi, D. Warner, K. Chibale, Synthesis and biological evaluation of 2-aminothiazole derivatives as antimycobacterial and antiplasmodial agents, Bioorg Med Chem Lett.; 2014, **24** (2), 560–564.

xxxi Y. Shan, H. Gao, X. Shao, J. Wang, X. Pan, J. Zhang, Discovery of novel VEGFR-2 inhibitors. Part 5: Exploration of diverse hinge-binding fragments via core-refining approach, Eur J Med Chem.; 2015, **103,** 80–90.

xxxii Y. Shan, C. Wang, L. Zhang, J. Wang, M. Wang, Y. Dong, Expanding the structural diversity of diarylureas as multi-target tyrosine kinase inhibitors, Bioorg Med Chem.; 2016, **24** (4), 750–758.

xxxiii X. Zhang, Z. Tang, X. Niu, Z. Li, X. Fan, G. Zhang, Selenium-catalyzed carbonylation of 2-aminothiazole with nitro aromatics to N-aryl-N′-2-thiazolylureas, Tetrahedron Lett.; 2016, **57** (47), 5266–5270.

xxxiv S. Dallakyan, A.J. Olson, Methods in Molecular Biology,; 2015.

xxxv O. Trott, A.J. Olson, Software news and update AutoDock Vina: improving the speed and accuracy of docking with a new scoring function, Efficient Optimization, and Multithreading, Journal of computational chemistry.; 2010, **31(2),** 455-461.

xxxvi V.M. Kumbar, M.R. Peram, M.S. Kugaji, T. Shah, S.P. Patil, U.M. Muddapur, K.G. Bhat, Effect of curcumin on growth, biofilm formation and virulence factor gene expression of Porphyromonas gingivalis, Odontology.; 2021, **109** (1), 18–28.

xxxvii D. Veeranna, L. Ramdas, G. Ravi, S. Bujji, V. Thumma, J. Ramchander, Synthesis of 1,2,3-Triazole Tethered Indole Derivatives: Evaluation of Anticancer Activity and Molecular Docking Studies, ChemistrySelect.; 2022, **7** (29), e202201758.

xxxviii A.K. Shiau, D. Barstad, P.M. Loria, L. Cheng, P.J. Kushner, D.A. Agard, G.L. Greene, The structural basis of estrogen receptor/coactivator recognition and the antagonism of this interaction by tamoxifen, Cell.; 1998, **95** (7), 927–937.

xxxix J. Nowakowski, C.N. Cronin, D.E. McRee, M.W. Knuth, C.G. Nelson, N.P. Pavletich, J. Rogers, B.-C. Sang, D.N. Scheibe, R. V Swanson, D.A. Thompson, Structures of the cancer-related Aurora-A, FAK, and EphA2 protein kinases from nanovolume crystallography., Structure.; 2002, **10** (12), 1659–1667.

xl C. Mazza, R. Breton, D. Housset, J.C. Fontecilla-Camps, Unusual charge stabilization of NADP+ in 17β-hydroxysteroid dehydrogenase, Journal of Biological Chemistry.; 1998, **273** (14), 8145–8152.

xli Y.-R. Wang, S.-F. Chen, C.-C. Wu, Y.-W. Liao, T.-S. Lin, K.-T. Liu, Y.-S. Chen, T.-K. Li, T.-C. Chien, N.-L. Chan, Producing irreversible topoisomerase II-mediated DNA breaks by site-specific Pt(II)-methionine coordination chemistry, Nucleic Acids Res.; 2017, **45** (18), 10861–10871.

xlii W. Tian, C. Chen, X. Lei, J. Zhao, J. Liang, CASTp 3.0: computed atlas of surface topography of proteins., Nucleic Acids Res.; 2018, **46** (W1)**,** W363–W367.

xliii S. Saha Roy, R.K. Vadlamudi, Role of estrogen receptor signaling in breast cancer metastasis., Int J Breast Cancer.; 2012, 654-698.

xliv M. Warner, S. Nilsson, J.-Å. Gustafsson, The estrogen receptor family, Curr Opin Obstet Gynecol.; 1999, **11** (3), 249–254.

xlv J.F. Couse, K.S. Korach, Estrogen receptor transcription and transactivation: Estrogen receptor knockout mice: what their phenotypes reveal about mechanisms of estrogen action., Breast Cancer Res.; 2000, **2** (5), 345–352.

xlvi A. Tang, K. Gao, L. Chu, R. Zhang, J. Yang, J. Zheng, Aurora kinases: novel therapy targets in cancers., Oncotarget.; 2017, **8** (14), 23937–23954.

xlvii R. Du, C. Huang, K. Liu, X. Li, Z. Dong, Targeting AURKA in Cancer: molecular mechanisms and opportunities for Cancer therapy, Mol Cancer.; 2021, **20** (1), 1-27.

xlviii D. Poirier, J. Roy, R. Maltais, A Targeted-Covalent Inhibitor of 17β-HSD1 Blocks Two Estrogen-Biosynthesis Pathways: In Vitro (Metabolism) and In Vivo (Xenograft) Studies in T-47D Breast Cancer Models., Cancers (Basel).; 2021, **13** (8), 1841.

xlix Ž. Skok, N. Zidar, D. Kikelj, J. Ilaš, Dual Inhibitors of Human DNA Topoisomerase II and Other Cancer-Related Targets, J Med Chem.; 2019, **63** (3) 884–904.

l V.M. Matias-Barrios, M. Radaeva, Y. Song, Z. Alperstein, A.R. Lee, V. Schmitt, J. Lee, F. Ban, N. Xie, J. Qi, N. Lallous, M.E. Gleave, A. Cherkasov, X. Dong, Discovery of New Catalytic Topoisomerase II Inhibitors for Anticancer Therapeutics, Frontiers in Oncology.; 2021, 3293.

Received on October 8, 2022